Mon. Not. R. Astron. Soc. **374,** 292–304 (2007) doi:10.1111/j.1365-2966.2006.11146.x

The star formation rate of Ca II and damped Lyman α absorbers at $0.4 < z < 1.3$

Vivienne Wild,[1]★ Paul C. Hewett[2] and Max Pettini[2]
[1]*Max Planck Institute for Astrophysics, Karl-Schwarzschild Str. 1, 85748 Garching, Germany*
[2]*Institute of Astronomy, University of Cambridge, Madingley Road, Cambridge CB3 0HA*

Accepted 2006 October 3. Received 2006 October 3; in original form 2006 July 14

ABSTRACT

Using stacked Sloan Digital Sky Survey (SDSS) spectra, we present the detection of [O II] λλ3727, 3730 nebular emission from the galaxies hosting Ca II absorption line systems and galaxies hosting Mg II-selected damped Lyman α (DLA) absorbers. Both samples of absorbers, 345 Ca II systems and 3461 Mg II-selected DLA systems, span the redshift interval $0.4 \leqslant z_{\rm abs} < 1.3$; all of the former and half the latter sample are expected to be bona fide DLAs. The measured star formation rate (SFR) per absorber from light falling within the SDSS fibre apertures (corresponding to physical radii of 6–9 h^{-1} kpc) is 0.11–0.14 $\mathrm{M}_{\odot}\ \mathrm{yr}^{-1}$ for the Mg II-selected DLAs and 0.11–0.48 $\mathrm{M}_{\odot}\ \mathrm{yr}^{-1}$ for the Ca II-absorbers. These results represent the first estimates of the average SFR in an absorption-selected galaxy population from the direct detection of nebular emission. Adopting the currently favoured model in which DLAs are large, with radii $\gtrsim 9\,h^{-1}$ kpc, and assuming no attenuation of the [O II] emission by dust, leads us to conclude that the SFR per unit area of Mg II-selected DLAs falls an order of magnitude below the predictions of the Schmidt law, which relates the SFR to the H I column density at $z \sim 0$. While DLA sightlines are known to contain little dust, the unknown geometry of the dust distribution in the galaxies causes the main uncertainty in our results.

The contribution of both DLA and Ca II absorbers to the total observed star formation rate density, $\dot{\rho}^*$, in the redshift range $0.4 < z < 1.3$, is small, $\lesssim$10 and $\lesssim$ 3 per cent, respectively. The result contrasts with the conclusions of Hopkins et al. that DLA absorbers can account for the majority of the total observed $\dot{\rho}^*$ in the same redshift range. The disagreement is a direct consequence of the much lower SFR per unit area we observe than predicted by the Schmidt law. Our results effectively rule out a picture in which DLA absorbers are the sites in which a large fraction of the total $\dot{\rho}^*$ at redshifts $z \lesssim 1$ occurs.

Key words: galaxies: ISM – quasars: absorption lines.

1 INTRODUCTION

Uncovering the physical properties of the host galaxies of strong quasar absorption line systems is a key topic in extragalactic astronomy today. These absorbers are expected to select galaxies based on gas cross-section, rather than luminosity, providing a complementary view of the galaxy population to that obtained from traditional stellar luminosity selected galaxy samples. However, with the possible exception of the common Mg II λλ2796, 2803 absorption line systems, the identification of large samples of absorption-selected objects with known emission properties has not been possible, despite considerable effort. A complete picture relating the gas cross-section, ionization state and chemical abundances of the interstellar media and gaseous haloes surrounding galaxies to the emission properties of the associated galaxy remains elusive.

At high redshift ($z \gtrsim 2$), observational efforts have focused on the highest neutral hydrogen (H I) column density systems, damped Lyman α systems (DLAs). These systems contain the majority of neutral gas at high redshifts and may provide the fuel reservoirs for subsequent star formation in galaxies (Lanzetta, Wolfe & Turnshek 1995). Emission, in general from Lyman α, from less than a dozen host galaxies of high-redshift DLAs has been detected and spectroscopically confirmed: a summary is given in Weatherley et al. (2005). Adopting only modest corrections to allow for the presence of dust, both detections and limits to the inferred star formation rates (SFRs) of these systems are relatively large, $\gtrsim 10\,\mathrm{M}_{\odot}\ \mathrm{yr}^{-1}$.

The small, inhomogeneous samples of counterpart galaxies have precluded direct estimates of the total SFR density ($\dot{\rho}^*$) of galaxies associated with high-redshift absorption systems; however, two

★E-mail: vwild@mpa-garching.mpg.de

methods have been used to obtain indirect estimates. Hopkins, Rao & Turnshek (2005) extrapolated the low-redshift relation between H I column density and SFR to high redshift; while Wolfe et al. (2003a, b) focused on the use of absorption from the fine-structure levels of the ground state of C II to estimate the SFR per unit area in DLAs and to calculate their contribution to $\dot{\rho}^*$ at high redshift. Both approaches involve significant assumptions and the conclusions of the two studies are only marginally consistent, with Wolfe, Gawiser & Prochaska (2003) advocating a larger contribution to the SFR density than Hopkins et al. (2005).

At lower redshifts ($z \lesssim 1$), galaxies associated with absorption-line systems are more readily observed because the angular separation between the galaxy and quasar is greater and deep imaging allows the detection of intrinsically fainter galaxies. Deep imaging and follow-up spectroscopic surveys of the fields of both DLAs and Mg II absorbers have revealed host galaxies with a wide range of morphological types and at varying impact parameters from the background quasar (Bergeron & Boisse 1991; Le Brun et al. 1993; Steidel, Dickinson & Persson 1994; Le Brun et al. 1997; Steidel et al. 1997; Rao et al. 2003; Chen, Kennicutt & Rauch 2005). Small samples, with incomplete spectroscopic follow-up, again hinder inference of the SFR density of absorption-selected galaxies. For a recent review on the nature of galaxies associated with Mg II absorbers see Churchill, Steidel & Kacprzak (2005).

Recently, Wild & Hewett (2005a) identified a new class of quasar absorption-line system selected by their strong Ca II λλ3935, 3970 absorption doublet[1] from quasar spectra in the Sloan Digital Sky Survey (SDSS). These rare (number densities ∼30 per cent of DLAs) absorption-line systems contain significant quantities of dust – $\langle E(B-V)\rangle \sim 0.1$ – in contrast to other samples of quasar absorption-line systems (Pettini et al. 1997; Murphy & Liske 2004; York et al. 2006). The dust and metal line properties of the Ca II absorbers strongly suggests they have H I column densities greater than the nominal limit for DLAs of $10^{20.3}$ atoms cm^{-2} (Wild, Hewett & Pettini 2006, hereafter WHP06).

The presence of strong Ca II absorption in absorption-line systems is of particular interest for studying the properties of the interstellar medium (ISM) of galaxies. Due to the convenient position of its resonance lines in the optical spectrum, Ca II has been well studied in the disc of the Milky Way (MW): its distribution is found to vary smoothly within the warm neutral medium and extend to a scaleheight of about 1 kpc from the plane of the disc (Edgar & Savage 1989; Welty, Morton & Hobbs 1996; Welsh et al. 1997; Hunter et al. 2006). Calcium is severely depleted on to dust grains in the MW (Savage & Sembach 1996) and, due to its second ionization potential of 11.87 eV being below the ionization potential of hydrogen, Ca II is a trace ionization state in the ISM of galaxies – most calcium is in the form of Ca III. The smoothness of the distribution, despite the sensitivity of gas phase Ca II to ionizing radiation fields and dust, have led to the suggestion that it traces warm neutral gas clouds within the MW, along with similarly depleted elements such as titanium (Hunter et al. 2006). Alternative explanations for the detection of strong Ca II lines in absorbers at $z \sim 1$ could be the destruction of dust grains, perhaps by shocks releasing calcium into the gas-phase, or lower radiation fields, perhaps within high-volume density clouds which afford a degree of self-shielding.

WHP06 investigated the dust content of the absorbers by measuring both the reddening of the background quasar and dust depletion patterns of different ions detected in stacked SDSS spectra. A dust-to-metal ratio similar to that of the MW was found, suggesting a higher degree of chemical evolution than in other quasar absorption-line systems (Vladilo 2004). The extent of depletion of refractory elements in the absorbers with highest equivalent width (EW) of the Ca II λ3935 line ($W_{\lambda 3935}$) was shown to equal that seen in the warm neutral medium of the MW, in contrast to average DLAs.

In this paper, we present the detection of the [O II] λλ3727,3730 emission doublet[2] associated with Ca II absorbers. The detection of [O II] confirms the presence of nearby star formation and allows, for the first time, a direct estimate of the average SFR in an absorption-selected galaxy population. In order to provide a comparison to a more commonly studied sample of absorption-line systems, we also analyse a sample of strong Mg II-selected absorbers in which 50 per cent are expected to be DLAs. Again, [O II] λλ3727, 3730 emission is detected.

The outline of this paper is as follows. In Section 2 we review the sample selection, extending our original Ca II and Mg II absorber samples to lower redshifts and lower signal-to-noise ratio (S/N) threshold. We also detail the methods used to create the composite spectra and measure the [O II] emission line luminosities. In Section 3, we present the measured [O II] line luminosities and discuss the magnitude of corrections required to convert these measurements into a total SFR for the absorber host galaxies. We calculate lower limits on the SFR per unit area of the absorbers, based simply on our observations and the size of the SDSS fibre aperture. Estimates of the SFR per unit area and the contribution of the absorber host galaxies to the volume averaged SFR density ($\dot{\rho}^*$) are derived in Section 4 which also includes a discussion of the combined uncertainties involved in these measurements. Finally, Section 5 discusses the implications of the observational results for the applicability of the Schmidt law (Schmidt 1959), relating the gas surface density to the SFR, to the absorbers and how our results compare with other recent work. Unless otherwise stated, a flat cosmology with $\Omega_\Lambda = 0.7, \Omega_M = 0.3, H_0 = 100\,h\,\mathrm{km\,s^{-1}\,Mpc^{-1}}$ and, where necessary, $h = 0.7$ is assumed throughout this paper.

2 METHOD

Quasar spectra were selected from the SDSS DR3 catalogue of Schneider et al. (2005) and supplemented with spectra in Data Release 4 (DR4, Adelman-McCarthy et al. 2006) main survey plates and spectroscopically classified as a quasar or high-redshift quasar.[3] Quasars in the sample were restricted to those with extinction-corrected point spread function (PSF) i-band magnitude ($m_{\mathrm{psf},i}$) brighter than 19.1. The redshift range of the quasars was restricted to $0.41 < z_{\mathrm{qso}} < 3.1$; the lower limit set to ensure that the presence of the Mg II λλ2796, 2803 doublet could be used to confirm the Ca II detections. To ensure our analysis was confined to relatively high-quality spectra, the quasar spectra were required to possess $\geqslant 3700$ good pixels ('NGOOD') and spectral S/N $\geqslant 6.0$ in both 'i' and 'r' bands.[4]

Quasar spectra showing evidence for broad absorption line (BAL) and strong associated absorption features were removed from the sample. This was achieved using a preliminary principal component based identification scheme similar to that of WHP06, followed by

[1] Vacuum wavelengths are used throughout this paper.

[2] Component vacuum wavelengths of 3727.09 and 3729.88 Å.

[3] 'SPECCLASS' equal to 3 or 4 in an SQL search of the DR4 catalogue

[4] A further ∼150 spectra suffering from a variety of artefacts, including many spectra in spectroscopic plates 426 and 946 included in the DR3 release, were removed from the sample following visual inspection.

confirmation through visual inspection. Comparison of our BAL and strong absorber catalogue to that of Trump, Hall & Reichard (2006) shows that the two agree extremely well; it was not possible to simply adopt the Trump et al. (2006) DR3 catalogue because our sample includes quasars in the DR4 release. While it is important to remove the 'BAL'-quasars from our sample to obtain accurate dust reddening estimates, none of the results described in the paper are sensitive to the exact identification scheme used. In the DR3 and DR4 samples of 27 010 and 7653 quasar spectra, 1812 and 573 objects, respectively, were identified as possessing BALs or strong associated absorption, leaving a combined sample of 32 278 quasar spectra in which absorption systems were sought.

2.1 The absorber sample

A matched-filter search was employed to detect Mg II λλ2796, 2803 absorption doublets with S/N $\geqslant 6$ over the redshift interval $0.4 < z_{\rm abs} < 1.3$ in the quasar spectra.[5] The search for Mg II doublets was restricted such that the absorbers appeared at wavelengths >1250 Å in the quasar rest frame, i.e. not in the Lyman α forest, and had redshifts $z_{\rm abs} < z_{\rm qso} - 0.03$. The quasar spectra were then searched independently for Ca II λλ3935, 3970 doublet absorbers with rest frame $W_{\lambda 3935} > 0.3$Å and S/N $\geqslant 4$ over the redshift interval $0.4 < z_{\rm abs} < 1.3$. The impact of imperfect removal of the OH skylines in the red half of the SDSS spectra was minimized by employing the routine of Wild & Hewett (2005b), with wavelength regions potentially occupied by known absorption lines masked. Further details of the line-finding procedure are given in WHP06.

The distribution of $z_{\rm abs}$(Mg II)$-z_{\rm abs}$(Ca II) shows a very strong excess of absorbers centred on zero-velocity difference with a dispersion of 70 km s^{-1}. An initial selection of 360 candidate Ca II absorbers was defined by selecting Ca II absorbers within a velocity difference of ± 200 km s^{-1} of a detected Mg II absorber. The fraction of spurious Ca II absorbers can be estimated directly from the incidence of apparent Ca II absorbers with velocity differences larger than ± 200 km s^{-1}. The level of contamination is well-determined and only 5 per cent of the sample of 360 candidate absorbers are predicted to be due to chance coincidence.

Absorption-line properties of the Fe II λ2600, Mg II λλ2796, 2803 and Mg I λ2853 features for all of the Mg II absorber candidates were calculated via a fully parametrized fit to the spectra.[6] The Ca II doublet was included for the subsample of Ca II absorbers. A continuum was fitted to the regions around the Mg II and Ca II lines and the corresponding portions of the quasar spectra were normalized by dividing by the continuum level. Gaussian doublets were then fitted to the normalized spectra using a maximum-likelihood routine; the position and linewidth of the doublet, and the relative strengths of the individual lines, were allowed to vary freely. Rest-frame EWs were calculated from the parameters of the Gaussian fits and errors estimated by propagation of the parameter errors derived during the maximum-likelihood fit.

Each candidate Ca II absorption-line system was inspected visually and 15 spurious detections were removed. Following Rao, Turnshek & Nestor (2006), Mg II systems were restricted to those with $1 < W_{\lambda 2796}/W_{\lambda 2600} < 2$ and $W_{\lambda 2796} > 0.6$ and only those systems with Fe II λ2600 and Mg II λ2796 lines detected with an S/N $\geqslant 3$ (see equation 1). This sample, referred to from now on as Mg II-selected DLA candidates, was selected to maximize the fraction of DLA systems it contains, about 50 per cent, thus providing a comparison to previous results for DLAs discussed in Section 1, and to the Ca II systems which are expected to be DLAs. Our final absorber catalogues contain 3461 Mg II absorption line systems and 345 Ca II absorbers in the redshift range $0.4 \leqslant z_{\rm abs} \leqslant 1.3$.

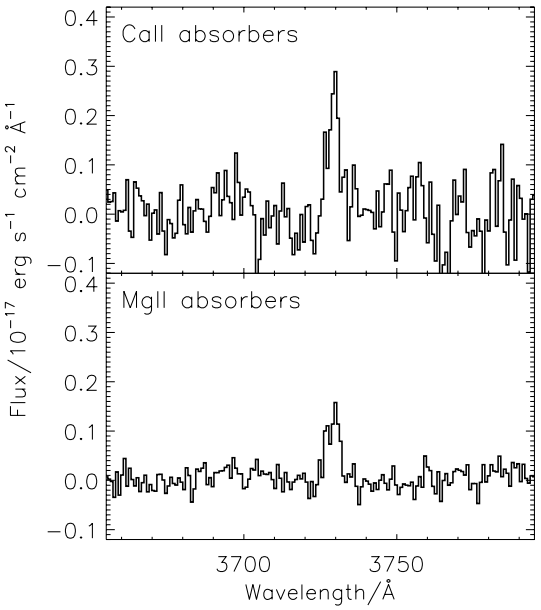

Figure 1. The wavelength region 3655–3795 Å of a composite of the 345 Ca II absorbers (upper Panel) and of a composite of 3461 Mg II absorbers (lower Panel) in the absorber rest frame. The individual spectra have simply been moved to the absorber rest frame, normalized and averaged together.

The samples are more extensive than those reported in WHP06 due to (i) the increased redshift interval searched, $z_{\rm abs} > 0.4$ compared to $z_{\rm abs} > 0.84$, (ii) the larger number of quasar spectra used by reducing the spectrum SNR threshold from 10.0 to 6.0 and (iii) the lower significance threshold for the detection of the Ca II absorbers, reduced from S/N > 5.0 to S/N > 4.0, subject to the presence of Mg II absorption within ± 200 km s^{-1}.

Before considering the detailed procedures employed to obtain measurements of the [O II] λλ3727, 3730 emission associated with the samples, it is worth stressing the potential of the SDSS spectroscopic data base for such investigations. The typical 1σ noise in the SDSS quasar spectra is $\sim 1 \times 10^{-17}$ erg cm^{-2} s^{-1} per pixel ($\Delta v = 69$ km s^{-1}), and detection limits for (close to) unresolved features in several hundred or more stacked spectra can easily reach 10^{-18} erg cm^{-2} s^{-1}. At redshifts of $z \sim 1$ such fluxes translate to unattenuated [O II] emission corresponding to SFRs of significantly below 1 $M_\odot$ yr^{-1}. Fig. 1 shows the wavelength region 3655–3795 Å of composites of the Ca II- and Mg II-selected DLA absorbers in the absorber rest frame; the individual spectra have simply been moved to the absorber rest frame, normalized and averaged together. The clear presence of the [O II] emission line is striking, including the partial resolution of the doublet.

2.2 Building the composite spectra

For the quantitative investigation of the [O II] emission line properties of the absorbers, the spectra were first corrected for the effects of

[5] The S/N is calculated from the combined detection of both members of the doublet.

[6] MPFIT, http://cow.physics.wisc.edu/~craigm/idl/, Craig Markwardt IDL library.

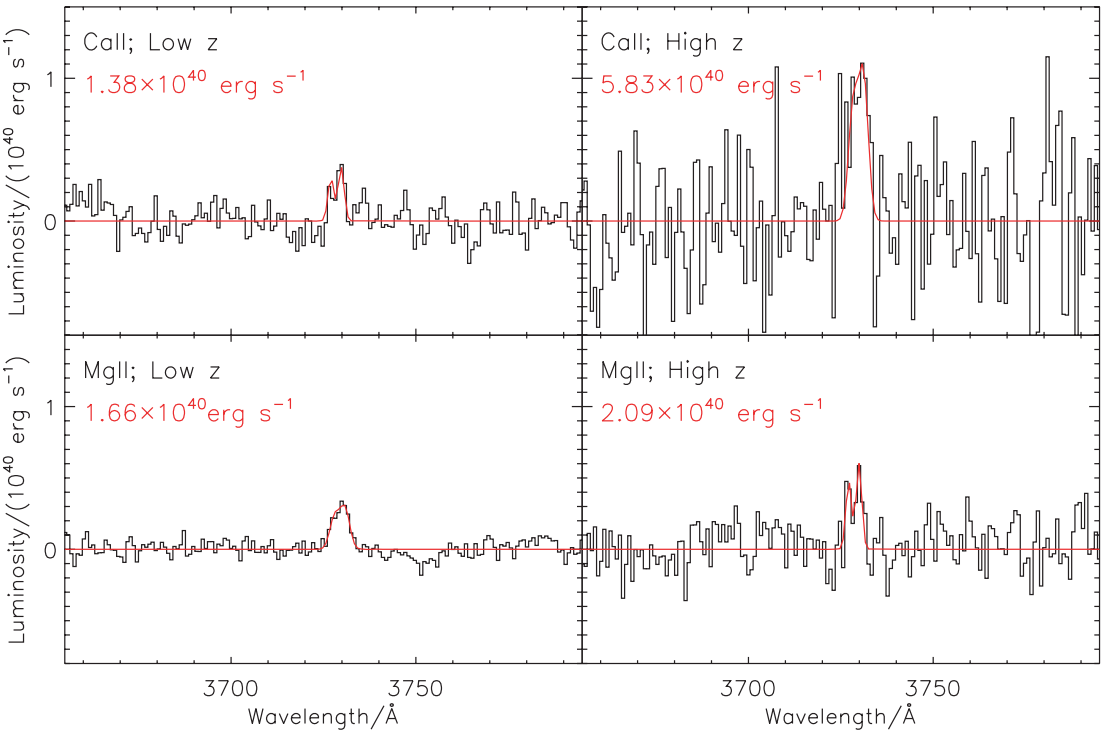

Figure 2. SDSS composite spectra of Ca II absorption line systems (top panel) and Mg II-selected DLA candidates (bottom panel) in the region of [O II] λλ3727, 3730 in redshift bins of $0.4 \leqslant z_{\rm abs} < 0.8$ (left-hand panel) and $0.8 \leqslant z_{\rm abs} < 1.3$ (right-hand panel). Flux from each contributing spectrum has been converted into luminosity before combining. Overplotted (in red lines) are Gaussian fits to the emission lines. Measured line luminosities from these line fits are given in each plot.

Galactic extinction, then moved to the absorber rest frame, without rebinning, correcting the flux into rest-frame per-Å units. Continua in the region of [O II] were defined using a running median filter (size 61 pixel) and subtracted from each spectrum. The residual spectra were weighted by the square of the luminosity distance to the absorber and combined into a composite using an arithmetic mean.[7]

The absorber sample covers an extensive redshift interval, over which it is believed the average SFR in galaxies changed significantly (Hopkins 2004). Composites were therefore created in two redshift bins, $z_{\rm abs}$ = 0.4–0.8 and 0.8–1.3. For the Ca II absorbers these redshift subsets were further split into two by $W_{\lambda 3935}$, because of the known variation of dust properties with strength of Ca II absorption (Wild & Hewett 2005a). An EW-limit of $W_{\lambda 3935} = 0.68$ Å was chosen for this division to match that used in WHP06 but the results reported below are not sensitive to the exact value of EW used. Unlike any of the Ca II absorbers, ∼0.2 per cent of the Mg II absorber spectra show detectable [O II] emission in individual spectra. However, the contribution to the mean [O II] luminosity of the absorber sample by these objects is small and the results of the paper are not dependent on the inclusion of the small percentage of such systems. The composite spectra in the region of the [O II] line are shown in Figs 2 and 3.

2.3 [O II] λλ3727, 3730 line fitting

In each composite spectrum the [O II] λλ3727, 3730 doublet was fitted with a double Gaussian with line ratio fixed at 4:5,[8] using a non-linear least-squares fitting routine, and line luminosities measured from the fitted Gaussian parameters. Whether or not a feature was detected was determined via its S/N (Hewett et al. 1985; Bolton et al. 2004, for a full derivation):

$$\mathrm{S/N} = \frac{\sum_i f_i^r u_i / \sigma_i^2}{\sqrt{\sum_i u_i^2 / \sigma_i^2}}, \qquad (1)$$

where f^r is the composite spectrum and σ is the flux error, u is a Gaussian line profile of position and width given by the fitted line parameters. A positive detection was defined to have an S/N > 3.0. Where a line was undetected, upper limits were placed for a single Gaussian line of σ twice the pixel resolution and detection limit of S/N = 3.0.

Table 1 presents the measured [O II] line luminosities and errors for each composite. From these values we make a few immediate observations. First, there is a significant difference between the samples split by redshift, particularly for the Ca II absorbers, which may be caused, in part at least, by aperture bias – less galaxy light falling within the fibre radius at low redshifts. Secondly, there appears to be a trend of increasing SFR with increasing $W_{\lambda 3935}$ in the

[7] In this situation, it is not possible to use a weighted mean due to the correlation between absorber redshift and S/N of the spectra: low-redshift absorbers can be detected in lower redshift quasars which have generally higher S/N spectra.

[8] The 4:5 line ratio is that predicted for $T = 10\,000$ K and electron density $N_{\rm e} = 200\,{\rm cm}^{-3}$ (Osterbrock 1989) and it provides a good fit to the composite [O II] λλ3727, 3730 doublet. The line strength measures are not sensitive to reasonable variations in the adopted line ratio.

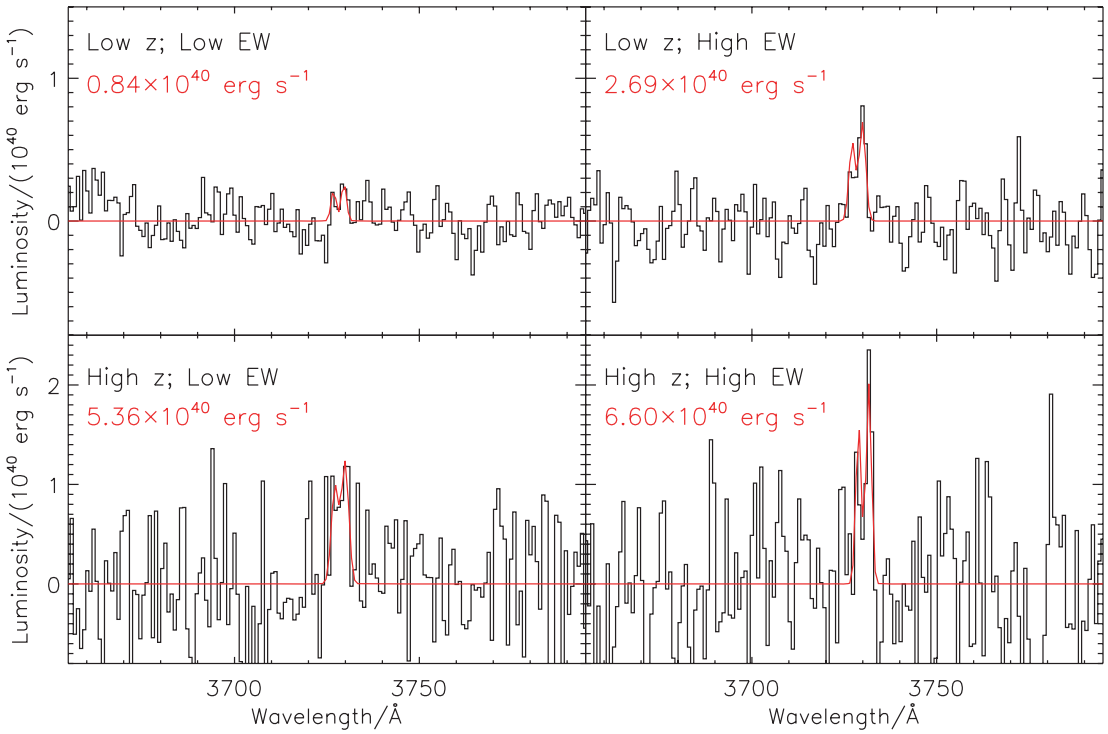

Figure 3. Same as Fig. 2 for the four subsamples of Ca II absorbers split by redshift and $W_{\lambda 3935}$. No line is formally detected in the top left-hand plot (S/N < 3). Note the change in *y*-axis scale between the upper and lower plots.

Table 1. Sample sizes, reddening, measured [O II] line luminosities, inferred SFRs before and after correction for dust, and dust obscuration bias effecting the observed population, for each Ca II composite spectrum and the two Mg II-selected DLA candidate composite spectra.

Sample	$N_{\rm abs}$	$E(B-V)$ (mag)	L[O II] (10^{40} erg s^{-1})	S/N	SFR ($M_\odot$ yr^{-1})	SFR^a ($M_\odot$ yr^{-1})	Dust bias^b [$E(B-V)_{\rm max}$]
Low z	215	0.036 ± 0.005	1.4 ± 0.2	5.9	0.09 ± 0.01	0.11 ± 0.02	0.24 (0.2)
High z	130	0.049 ± 0.004	5.8 ± 0.6	5.8	0.38 ± 0.04	0.48 ± 0.05	0.45 (0.25)
Low z, low EW	153	0.029 ± 0.006	<0.9	3.0	<0.06	<0.07	0.20 (0.2)
Low z, high EW	62	0.051 ± 0.009	2.7 ± 0.4	6.6	0.18 ± 0.03	0.22 ± 0.03	0.33 (0.2)
High z, low EW	74	0.036 ± 0.006	5.4 ± 1.3	4.3	0.35 ± 0.09	0.41 ± 0.10	0.34 (0.25)
High z, high EW	56	0.066 ± 0.007	6.6 ± 1.2	5.0	0.43 ± 0.08	0.58 ± 0.10	0.56 (0.25)
Low z, Mg II	1291	–	1.7 ± 0.06	15.2	0.11 ± 0.004	–	–
High z, Mg II	2170	–	2.1 ± 0.3	7.0	0.14 ± 0.02	–	–

[a]Corrected for dust attenuation at [O II], based on $E(B-V)$ derived from reddening of the background quasar; [b]fraction of the total population of Ca II absorbers lost due to dust obscuration of the background quasar sample; this calculation is only performed for absorbers with $E(B-V)$ less than the value given in brackets.

low-redshift Ca II subsample, but no trend is detected at high redshift, although the errors are large. Again, if stronger Ca II absorbers were more likely to be found at smaller impact parameters from the galaxy centre, the difference could be a manifestation of aperture bias. Due to the large errors and evidently weak, or non-existent, trends with equivalent width, the remainder of this paper will focus on the samples split by redshift only.

3 STAR FORMATION RATES

We convert the [O II] line luminosities into instantaneous SFRs, listed in column 6 of Table 1, using the relation of Kewley, Geller & Jansen (2004):

$$\mathrm{SFR([O\,II])(M_\odot\ yr^{-1})} = 6.58 \pm 1.65 \times 10^{-42} L([\mathrm{O\,II}]), \qquad (2)$$

where [O II] luminosity is measured in erg s^{-1}. The errors on our measured line fluxes and the uncertainty associated with the SFR conversion have been propagated in the usual way. In the following subsections we discuss three correction factors which must be applied to these values in order to estimate the true average SFR of absorber host galaxies. The first two are caused by dust within the ISM of the absorber host galaxy, the third by the finite aperture of the SDSS fibres.

3.1 Dust corrections to Ca II absorbers

While the dust content of the Mg II-selected DLA candidates is negligible (WHP06), it is necessary to correct our measured SFRs for the effect of dust in the Ca II host galaxies. This correction is twofold. First, the [O II] photons are absorbed by dust grains, thus reducing the line flux emitted from the galaxy. Secondly, the dust obscures the background quasars, thus reducing the total redshift path available to find Ca II absorption line systems in the survey over that naively expected. To estimate the magnitude of both effects we require the

extinction as a function of wavelength caused by the dust. This can be achieved from the measured reddening in each subset, by assuming the form of the extinction curve and the total-to-selective extinction ratio [$R_V \equiv A_V/E(B-V)$]. In what follows we assume the dust content as measured from the absorption line of sight is applicable to that obscuring the nebular emission line region. In Section 4.4.2, we discuss the potential problems with this assumption given the likely complicated geometry of the dust distribution within galaxies.

For a full description of our method to measure dust reddening in the absorbers see WHP06; a brief description is given here. High-S/N quasar template spectra are created by combining the spectra of all quasars in our input sample which do not contain known Mg II systems, a total of 22 727 quasar spectra with $0.35 < z_{\rm qso} < 3.15$. The template spectra are created in redshift bins of $\Delta z_{\rm qso} = 0.1$. Each quasar spectrum containing an intervening absorption-line system is then divided by a suitably normalized high-S/N quasar template spectrum. Each residual spectrum is then moved to the rest frame of the absorber and all residual spectra in the subsample are combined using an arithmetic mean. The resulting residual spectrum is fitted with the Large Magellanic Cloud (LMC) reddening curve[9] of Pei (1992) and the resulting $E(B-V) \equiv A_B - A_V$ values are given in the third column of Table 1.

The formal errors on this fit are small and the dominant source of error arises from the intrinsic variation in quasar spectral energy distributions (SEDs). This error is estimated via 10 000 Monte Carlo simulations drawing a random subset of quasar spectra equal in size to the subset of absorbers. A random absorber redshift is assigned to each quasar spectrum and the above method repeated to estimate the reddening of this simulated sample of absorbers. Repeating 10 000 times, the 68th percentiles of the final reddening distribution are taken to provide the errors quoted in the third column of Table 1. Again, further details on this error calculation are provided in WHP06.

3.1.1 [O II] line attenuation

The attenuation of light due to dust at the wavelength of [O II] is calculated from the measured $E(B-V)$ values in the absorption line systems, and the assumed extinction curve. The resulting dust attenuation corrected [O II] SFRs are given in column 7 of Table 1. Again, the errors have been propagated in the usual way. In the calculation, we have assumed that the photons from the star-forming regions are passing through the same quantity and type of ISM as the light from the background quasar, an assumption that will not be correct in detail. However, without further information on the nature of the relation between the absorbers and host galaxies it is difficult to improve on this assumption. The effect on our results of possible enhanced extinction in the nebular emission line regions is discussed further in Section 4.4.2.

3.1.2 Dust obscuration of the background quasars

The second effect of dust in the absorber is to obscure the background quasars, meaning that fewer Ca II absorption-line systems are found in a magnitude-limited quasar sample than if the absorbers did not contain dust. The method of correction for this 'dust obscuration bias' is discussed in detail in WHP06, but given the importance of the correction we include a revised description of the procedure in Appendix A.

The fraction, (b), of the total Ca II absorber population lost due to dust obscuration bias is given in the final column of Table 1 for each Ca II sample. To obtain the true number of Ca II absorbers which would have been observed had they contained no dust, the observed number is divided by $(1-b)$. The redshift, as well as the dust content, of the absorbers has a large effect on the extent of the bias due to the shape of the dust extinction curves – the strongest attenuation is at small wavelengths; higher redshift absorbers therefore cause greater extinction to the background quasar. The smallest correction factor applies to the least dusty absorbers at the lowest redshift. Conversely for the absorbers with $W_{\lambda 3935} > 0.68$ and $0.8 \leqslant z_{\rm abs} < 1.3$ we are in fact only observing 44 per cent of the total number of Ca II absorbers with $E(B-V) < 0.25$. As argued in WHP06, these correction factors are very well determined. However, as discussed in Appendix A, there is an important caveat; we are unable to correct reliably for absorbers with an $E(B-V) > 0.2$ and >0.25 for the low- and high-redshift samples, respectively, because our observations have little or no sensitivity to absorbers with such values of $E(B-V)$.

3.2 Non-DLA contamination of Mg II-selected DLA sample

Bias due both to [O II] line attenuation and the obscuration of background quasars is minimal for the Mg II-selected DLA candidate sample given the very low dust content (see WHP06) and we have not applied any corrections to the measured line fluxes. One uncertainty in the implied SFR of DLAs from our analysis lies in the contribution made by the 50 per cent non-DLA contaminants to this sample. An estimate of the SFR of these contaminants can be calculated by measuring the SFR found in Mg II absorbers which fall out of the predicted DLA Fe II/Mg II EW ratio range, but still with $W_{\lambda 2796} > 0.6$ Å. In these absorbers we measure SFRs of 31(57) per cent those found in the low- (high-) redshift Mg II-selected DLA candidate sample, producing corrections to the SFRs quoted in the final two rows of Table 1 of a factor of 1.69(1.43). We note that this method of estimating the correction factors is only approximate and the associated uncertainties are discussed further in Section 4.4.

3.3 Aperture corrections

The final correction factor which must be applied to our measured SFRs in both the Ca II and Mg II samples is for the finite aperture of the SDSS fibre, which is centred on the background quasar and not on the host galaxy of the absorber. The fibre may be covering a fraction of empty sky, which has implications for our measures of SFR per unit area of the absorbers; or it may be missing a fraction of the galaxy light, with implications for our estimate of the SFR per absorber; or both.

For ease of reference, Fig. 4 depicts the proper transverse distance covered by a 3 arcsec diameter fibre as a function of redshift. Atmospheric seeing will cause a blurring of the discontinuity at the edge of the fibre, but in practice star formation occurring within $\sim 17/2 = 8.5\,h^{-1}$ kpc from the line of sight to the quasars will contribute to the observed SFR for our highest redshift absorbers. At the lowest redshifts in our sample this is reduced to $\sim 14/2 = 7\,h^{-1}$ kpc. The fibres cover a relatively large area, comparable to the size of the star forming extent of a galaxy at these redshifts (Ferguson et al. 2004), but a smaller area than the likely extent of, for example, Mg II or H I

[9] WHP06 found that the LMC reddening curve provided the best fit to the combined quasar residual spectra, although the derived values of $E(B-V)$ are not sensitive to the exact choice of extinction curve.

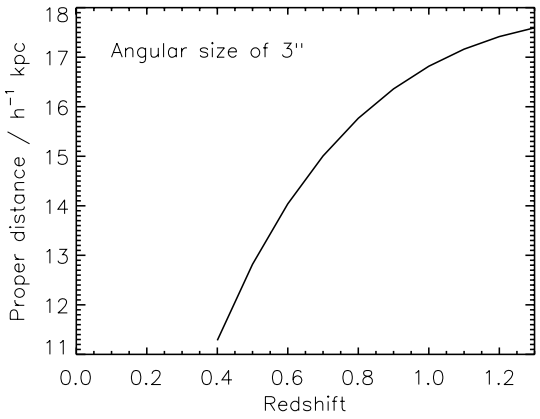

Figure 4. Proper transverse distance covered by a 3 arcsec diameter fibre as a function of redshift, for the ΛCDM cosmology used in this paper with $H_0 = 100\,\mathrm{km\,s^{-1}\,Mpc^{-1}}$.

haloes/discs surrounding the galaxies. To calculate many quantities of interest, such as SFR density per unit volume as a function of redshift, $\dot{\rho}^*(z)$, information on the size of the absorbers is required and this aspect of the discussion is deferred to Section 4.

3.4 Summary of observational results

Table 1 summarizes the principal observational result of this paper relating to the integrated SFR for the absorbers, i.e. the determination of the observed average SFR for the Ca II absorbers and the Mg II-selected DLA candidates. In the remainder of this section we look at the SFR per unit area of the absorber host galaxies, for which a hard lower limit can be obtained by dividing the observed average SFR per absorber by the area of the spectroscopic aperture at the absorber redshift. The lower limit arises due to the uncertainty as to the fraction of the fibre which falls on blank sky.

3.4.1 Mg II-selected DLAs

By dividing the SFRs given in the final two rows of Table 1 by the proper area of the fibre at the central redshift of the samples, and correcting for the 50 per cent of non-DLAs in the sample as discussed above, we obtain limits on the SFR per unit area of DLAs. The limits are $\gtrsim 12 \pm 0.4 \times 10^{-4}$ and $\gtrsim 9 \pm 1 \times 10^{-4}\,h^2\,\mathrm{M_\odot\,yr^{-1}\,kpc^{-2}}$ for the low-z ($\langle z\rangle \approx 0.6$) and high-$z$ ($\langle z\rangle \approx 1.0$) samples.

To put these limits into context, we compare with the Kennicutt parametrization of the Schmidt law (Schmidt 1959; Kennicutt 1998a,b), which relates the surface densities of neutral gas and SFR in galaxies:

$$\sum_{\mathrm{SFR}} = 2.5 \times 10^{-4} \times \left[\frac{N(\mathrm{H\,I})}{1.25 \times 10^{20}\,\mathrm{cm^{-2}}}\right]^{1.4} \quad (3)$$

above a critical H I column density, $N_\mathrm{c} = 5 \times 10^{20}\,\mathrm{cm^{-2}}$, where $\sum_{\mathrm{SFR}}$ is in units of $\mathrm{M_\odot\,yr^{-1}\,kpc^{-2}}$. A distribution function for the H I column densities of the absorbers is thus required to predict their SFR per unit area. In fact, the combination of the critical threshold value N_c for the onset of star formation, combined with the non-linear dependence of the SFR on column density, means that simply evaluating equation (3) for $\langle N(\mathrm{H\,I})\rangle$ produces an answer accurate to better than 10 per cent.

Taking the distribution of H I column densities for DLAs at $1.7 < z < 2.2$ of Prochaska, Herbert-Fort & Wolfe (2005) results in a mean column density of $6.6 \times 10^{20}\,\mathrm{cm^{-2}}$. The mean is insensitive both to the exact form of the acceptable functional fits given in Prochaska et al. (2005) and the upper cut-off in H I column density between 10^{22} and $10^{23}\,\mathrm{cm^{-2}}$. The latter behaviour is due to the steep decline in the number of systems at very high column densities. Unfortunately, at $z < 2$, the redshift range applicable to our systems, significant uncertainty in the predicted SFR per unit area for the absorber populations comes about because of the poorly determined distribution of N(H I). Rao et al. (2006) find that the mean N(H I) is somewhat higher than assumed above, $\langle N(\mathrm{H\,I})\rangle = 1.27 \pm 0.36 \times 10^{21}\,\mathrm{cm^{-2}}$ for DLAs with $0.11 < z < 0.9$, and $1.07 \pm 0.23 \times 10^{21}\,\mathrm{cm^{-2}}$ for DLAs with $0.9 < z < 1.65$.

The Rao et al. (2006) mean column density $\langle N(\mathrm{H\,I})\rangle$ corresponds to a SFR per unit area of $13.1 \pm 5.2 \times 10^{-3}$ and $10.3 \pm 3.1 \times 10^{-3}\,h^2\,\mathrm{M_\odot\,yr^{-1}\,kpc^{-2}}$ according to equation (3), for their low- and high-redshift bins, respectively. These values are factors of 11 ± 4 and 11 ± 3 higher than the lower limits we deduced for our low- and high-z samples (the errors here are dominated by the uncertainty in $\langle N(\mathrm{H\,I})\rangle$). For comparison, the high-redshift $\langle N(\mathrm{H\,I})\rangle$ value of Prochaska et al. (2005) results in a predicted SFR per unit area for DLAs of $5.2 \times 10^{-3}\,h^2\,\mathrm{M_\odot\,yr^{-1}\,kpc^{-2}}$. This is still four (six) times greater than the derived lower limit in the low- (high-) z Mg II-selected DLAs.

Does the mean H I column density of DLAs apply to our Mg II-selected sample? These absorbers were selected to maximize the DLA fraction they contain and allowance was made to correct the observed SFR for contamination by non-DLAs (Section 3.2). The results of Rao et al. (2006) are based on follow-up N(H I) observations of a sample of Mg II-selected systems very similar to that used here and it would be very surprising if the properties of our Mg II absorber sample were significantly different from those studied by Rao et al. (2006).

3.4.2 Ca II absorbers

In the case of the Ca II absorbers, dividing the SFRs by the proper area of the fibre at the central redshift of the samples results in limits for the SFR per unit area of $\gtrsim 7\ (21) \times 10^{-4}\,h^2\,\mathrm{M_\odot\,yr^{-1}\,kpc^{-2}}$ for the low- (high-) z samples, respectively, after correcting the SFRs for attenuation of the [O II] line by dust.

It is difficult to compare these results to those predicted by the Schmidt law, due to the very few systems currently with both Ca II and N(H I) measures, particularly for the high $W_{\lambda 3935}$ systems. While the Ca II absorbers are expected to have N(H I) values above the nominal limit for DLAs, the comparison to predicted SFRs per unit area of DLAs should be treated with caution.

In the following section, we discuss the magnitude of corrections applicable to these values caused by portions of the fibre aperture covering blank sky, and convert the measured lower limits into absolute SFR per unit area values for the absorbers. Here we simply note that the corrections are expected to be small, particularly in the case of the Mg II-selected DLAs.

4 ABSORBER STAR FORMATION PROPERTIES

In this section, we use results of imaging surveys of DLAs to estimate their average extent and thus assess the magnitude of corrections applicable to our observed SFRs within the fibre aperture. The discussion in this section is predicated on the assumption that the SFR per unit area is determined entirely by the Schmidt law

via the H I column density, as specified in equation (3). If DLAs at $z \lesssim 1$ are caused by large gas discs surrounding a central galaxy, the absolute SFR per unit area observed through the SDSS fibre aperture can be predicted from the mean N(H I) of the population and, furthermore, we can estimate the contribution of the host galaxies to the star formation rate density ($\dot{\rho}^*$) of the Universe. Discussion of scenarios in which the relative location of star formation and absorption within a galaxy/halo system, and/or failure of the Schmidt law, impact greatly on our results follows in Section 5.

4.1 Physical size of absorbers

In the case of DLAs, imaging of host galaxies at $z \lesssim 1$ suggests they may occur in haloes or discs that extend out as far as $\sim 25\,h^{-1}$ kpc from the host galaxy (e.g. Chen & Lanzetta 2003; Rao et al. 2003; see table 2 of Zwaan et al. 2005 for a recent compilation). The mean observed impact parameter between DLAs and absorber host galaxies is $\sim 9\,h^{-1}$ kpc (table 2 of Zwaan et al. 2005). Assuming a simple circular geometry for the absorbers this corresponds to a typical absorber radius[10] of $\simeq 13\,h^{-1}$ kpc, assuming covering factors of unity. Comparatively, from direct H I observations of local galaxies, Zwaan et al. (2005) predicted a very similar mean impact parameter of $\sim 7\,h^{-1}$ kpc.

We therefore adopt $13\,h^{-1}$ kpc as the predicted extent from the centre of the host galaxy of absorbing clouds which give rise to DLAs. Adopting the measured value of $\mathrm{d}P/\mathrm{d}z = 0.079 \pm 0.019$ (Rao et al. 2006) for DLA absorbers at low redshifts, the estimated size leads to absorber space densities of 0.027 (0.022) h^3 Mpc^{-3} for our low- and (high-) redshift samples (equation 5).

We turn now to the Ca II absorbers. Without any direct observations of host galaxies, or information on how far Ca II extends into the gaseous haloes surrounding galaxies, we must make some assumption about their size. In WHP06 strong arguments are given that Ca II absorbers have N(H I) values above the nominal limit for DLAs and, as such, make up a subsample of DLAs. Their high dust and metal contents suggest a scenario in which Ca II absorbers exist closer to the central galaxy, possibly with a significant fraction lying within the star forming region of the galaxy. The values of $\mathrm{d}P/\mathrm{d}z(W_{\lambda 3795} > 0.5$ Å) for the Ca II absorbers, correcting for those missed from the sample due to dust obscuration bias, are 0.019 and 0.025 for our low- and high-redshift samples (WHP06 and see Section 4.3.1). Taking the same space densities as for the DLA absorbers and simply scaling the cross-sections according to the difference in the observed $\mathrm{d}P/\mathrm{d}z$ for the two absorber populations gives radii for Ca II absorbers of 0.49 (0.56) times those of DLAs, or 6.4 (7.3) h^{-1} kpc for the low- (high-) z samples.[11] We note that the difference in size for the two redshift intervals is not significant given the combined errors on number density for both the DLAs and Ca II absorbers.

4.2 SFR per unit area

Given the physical size of the absorbers we can calculate their actual SFR per unit area, within our assumed geometrical model, for which lower limits were calculated in Section 3.4.

[10] The mean observed impact parameter is about two-thirds of the maximum radius, assuming the absorbers present simple circular cross-sections.

[11] Despite the different method used to estimate the halo sizes of Ca II absorbers, the resulting size remains very similar to that suggested in WHP06.

Beginning with the Mg II-selected DLA candidates, placing 6–9 h^{-1} kpc radius circles (i.e. the SDSS spectroscopic fibres, see Section 3.3) at random across a second circle of radius $13\,h^{-1}$ kpc (i.e. the gaseous haloes or discs), such that the impact parameter between the centre of the circles never exceeds the radius of the second circle, and summing the fraction of area falling outside the absorber boundary (i.e. on blank sky) leads to aperture corrections of 1.16 and 1.21 for low- and high-z samples, respectively. Thus, the SFR per unit area of Mg II-selected DLA candidates derived in Section 3.4 can be increased only to $14 \pm 0.5(11 \pm 1.6) \times 10^{-4}\,h^2\,\mathrm{M}_\odot\,\mathrm{yr}^{-1}\,\mathrm{kpc}^{-2}$ and a large discrepancy between the conventional Schmidt relation and our observations remains.

Adopting the estimates for the size of the Ca II absorbers leads to an aperture correction of 1.59 (1.69) for the low- (high-) z samples. These corrections lead to a SFR per unit area of $11(36) \times 10^{-4}\,h^2\,\mathrm{M}_\odot\,\mathrm{yr}^{-1}\,\mathrm{kpc}^{-2}$, i.e. very similar to the Mg II-selected DLA candidates at low redshift, but four times higher in the high-redshift sample. *If* the mean H I column of Ca II absorbers is equal to that of DLAs with $1.7 < z < 2.2$, the high-redshift Ca II absorber host galaxies have SFRs per unit area closer to that predicted by the Schmidt law, while at low redshifts an order of magnitude discrepancy remains.

4.3 The global SFR density

The global SFR density of the universe has now been measured by many surveys out to high redshift. The general consensus is that, as we look back in time, the SFR density increases by about one order of magnitude from $z = 0$ to 1, and remains approximately constant at higher redshifts up to $z \sim 5$ (Bouwens & Illingworth 2006). Hopkins (2004) has provided a power-law fit to the data at $z < 1$:

$$\log \dot{\rho}^* = 3.29 \log(1+z) - 1.8, \tag{4}$$

where $\dot{\rho}^*$ is in units of $\mathrm{M}_\odot\,\mathrm{yr}^{-1}\,\mathrm{Mpc}^{-3}$ and $H_0 = 70\,\mathrm{km\,s^{-1}\,Mpc^{-1}}$. In our low- (high-) z bins the average SFR density of the universe is thus $\log \dot{\rho}^* \simeq -1.13$ (-0.81) or, with $\dot{\rho}^*$ in units of $h^3\,\mathrm{M}_\odot\,\mathrm{yr}^{-1}\,\mathrm{Mpc}^{-3}$, $\log \dot{\rho}^* \simeq -0.66(-0.35)$. From now on all $\dot{\rho}^*$ values will be quoted in the latter units.

Adopting either a physical size or a space density for the Ca II- and Mg II-selected DLA absorbers, and assuming the star formation is uniformly distributed (on scales similar to the fibre size) within the high column density gas, as required by the Schmidt law, we can estimate the contribution to the global SFR density of the universe from the host galaxies of each class of absorbers.

4.3.1 Cross-sectional area and comoving space density of the absorbers

The observed redshift number density ($\mathrm{d}P/\mathrm{d}z$) of absorbers provides a joint constraint on their size and space density. For absorbers with cross-sectional area, S, and comoving number density, $n(z)$, their number per unit redshift is given by (Peebles 1993; Hogg 1999):

$$\frac{\mathrm{d}P}{\mathrm{d}z} = Sn(z)\frac{c}{H_0}\frac{(1+z)^2}{\sqrt{\Omega_\mathrm{M}(1+z)^3+\Omega_\Lambda}}. \tag{5}$$

The $\mathrm{d}P/\mathrm{d}z$ of the whole Ca II absorber population, i.e. correcting for dust obscuration bias (Section 3.1.2), is obtained by multiplying the observed $\mathrm{d}P/\mathrm{d}z$ by the fraction lost due to dust bias (final column of Table 1). For the low- and high-redshift samples we

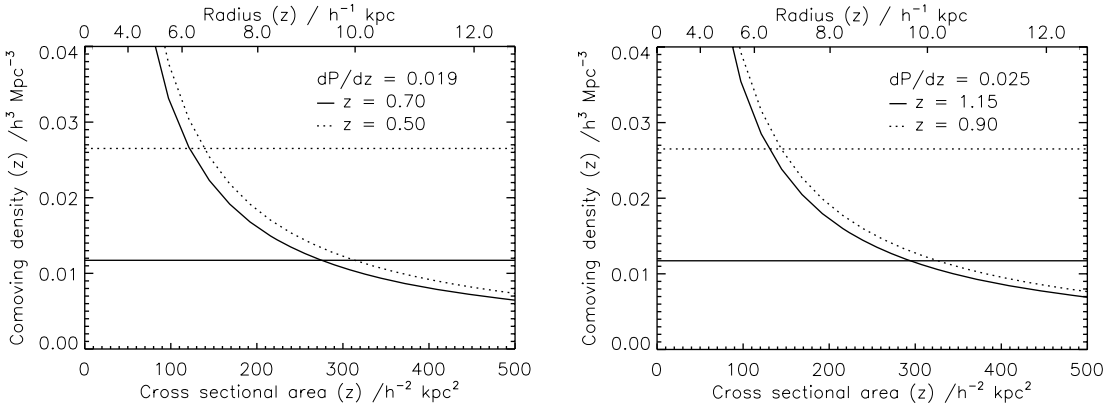

Figure 5. Combined constraints on cross-sectional area and comoving number density, given the measured dP/dz of the Ca II absorption-line systems corrected for those missed from the sample due to dust obscuration bias. Left-hand panel: low-redshift sample; right-hand panel: high-redshift sample. In each plot, the constraints are shown for two different redshifts within the redshift bin. The horizontal lines are comoving number densities of galaxies, at $z \sim 0$, with $M > M^* + 1$ and $M > M^* + 2$, where M^* is the 2dFGRS characteristic magnitude (see the text).

find dP/d$z(W_{\lambda 3795} > 0.5$ Å$) = 0.019$ and 0.025, respectively[12] (see WHP06 for a detailed method). In Fig. 5, we plot the combined constraint on comoving number density and cross-sectional area of the dust bias corrected Ca II absorber samples, given their respective redshift number densities. The constraints for two different redshifts within each redshift interval are plotted, although the change within a bin is not large.

To provide reference points, the $z \sim 0$ space density of galaxies with B-band magnitudes, $M > M^* + 1.0$ and $M > M^* + 2.0$ are indicated by horizontal lines. $M^* = -19.79 + 5\log_{10}(h)$ and $\phi^* = 0.00159\,h^3\,\mathrm{Mpc}^{-3}$, the characteristic magnitude (on the Vega-system) and normalization of the luminosity function, are taken from the rest-frame B-band Schechter function parametrization of the 2dF Galaxy Redshift Survey (2dFGRS, Madgwick et al. 2002).

4.3.2 *Contribution of absorber host galaxies to* $\dot{\rho}^*$

Starting with the Ca II absorbers, within the errors, the space density estimates of $0.027(0.022)\,h^3\,\mathrm{Mpc}^{-3}$ (Section 4.1), for the low- (high-) z samples, are consistent with zero evolution and are similar to the space density of galaxies brighter than $M^*_{\rm 2dF} + 2$.

Given the small impact parameters expected for the Ca II absorbers within our assumed model for the relative configuration of star formation and absorbing gas, the central host galaxy is expected to fall within the fibre aperture essentially all the time (Fig. 4). The fibre aperture correction factor (that quantifies the host galaxy emission line flux lying outside the fibre diameter) is 1.32(1.25) for the low- (high-) z samples. The volume averaged SFR density of the absorber host galaxies, obtained from the product of the SFR, the space density and the aperture corrections, is then $\log\dot{\rho}^* \simeq -2.43(-1.89)$. Comparing to equation (4) these values represent only 2(3) per cent of the total SFR density in the universe at the same redshifts.

Turning now to the Mg II-selected DLA absorbers, dP/dz is a factor 3 to 4 larger and, unless the DLAs possess a much higher space density than that of the Ca II absorbers, allowing them to be considerably smaller, their physical extents are such that a significant aperture correction is necessary in order to allow for the absorber gas that falls outside the 3-arcsec SDSS fibre aperture. Adopting the absorber size estimate of $13\,h^{-1}$ kpc, and hence space density, from Section 4.1 leads to aperture corrections of 3.9(2.9) for the low- (high-) z samples, respectively. Taking the measured SFR for the Mg II-selected DLA candidate sample then leads to values of $\log\dot{\rho}^* \simeq -1.72(-1.91)$. These values correspond to ∼9(3) per cent of the SFR density in the universe at $\langle z\rangle \simeq 0.6$ and $\langle z\rangle \simeq 1.0$, respectively.

It is not possible to explain the small contributions to the global SFR density by simply appealing to an underestimate of the size of the absorbers in Section 4.1. Once absorber size is comparable to or larger than the fibre-size (as in all examples here), and *assuming the Schmidt law holds*, changes in the assumed absorber size make no significant difference to the value of $\dot{\rho}^*$. This follows from $\dot{\rho}^*$ being proportional to the product of the comoving number density and aperture correction:

$$\dot{\rho}^* \propto \langle\mathrm{SFR}\rangle \times n(z) \times A$$
$$\propto \langle\mathrm{SFR}\rangle \times \frac{\mathrm{d}P/\mathrm{d}z}{S} \times A, \quad (6)$$

where $\langle$SFR$\rangle$ is the SFR per absorber, A is the aperture correction factor, $n(z)$ the comoving number density, S the area of the absorber and dP/dz is fixed by observation. In the limit that the size of the absorber (and star formation region) is greater than the fibre aperture, as S increases the aperture correction increases proportionately and $\dot{\rho}^*$ remains constant.

Our results for the $\dot{\rho}^*$ of Mg II-selected DLA candidates are directly comparable to those of Hopkins et al. (2005) who concluded that DLAs are responsible for as much as 80 per cent of the SFR density of the universe at similar redshifts to those considered here. The dramatic discrepancy between our study and theirs arises directly from the assumption by Hopkins et al. that the local Schmidt relation holds for DLA absorbers. Assuming the mean N(H I) for our Mg II-selected DLAs from Rao et al. (2006), as appropriate for a direct comparison between the results, we observe a SFR per unit area of $\lesssim$10 per cent of that expected were the Schmidt law to apply.

4.4 Summary of uncertainties

For each of our absorber samples potential sources of uncertainty in our analysis have been made clear throughout this paper. The final SFR measurements presented in Table 1 include associated

[12] Strictly speaking these are lower limits to the true number densities, as we are unable to correct for dust obscuration bias above the $E(B-V)_{\rm max}$ values given in Table 1.

line-measurement errors, the error on the conversion from [O II] luminosity to SFR and, in the case of the Ca II absorbers, the error on the dust attenuation correction estimated from the reddening of the background quasar continuum. In this subsection, we combine these errors with additional uncertainties in our calculations to produce an estimate of the reliability of our key results.

4.4.1 *Star formation rates from [O II] emission*

Kewley et al. (2004) presented a comprehensive analysis of the dependence of the [O II]-derived SFR in systems with an extended range of physical properties, including objects with SFRs significantly lower than those we measure for the absorber sample. Given the known low metallicity of DLA gas, the adopted Kewley et al. (2004) relation applies for systems with a mean metallicity that may be higher than that of the absorber populations. Applying a correction for metallicity would *decrease* the inferred SFR for a given [O II]-luminosity, increasing the disagreement between our observations and predictions based on the application of the Schmidt law. As very few absorption systems have measured emission-line abundances, and the link between absorption- and emission-line metallicities therefore remains unclear, it is not possible to assess this effect further at this stage.

4.4.2 *Dust attenuation of the [O II] emission*

In calculating the SFR of the Mg II-selected DLAs we have not made any correction for dust attenuation of the [O II] line, because of the very low reddening detected in Mg II absorbers by WHP06. Specifically, for an equivalently defined sample we found an $E(B-V)$ of 0.008 ± 0.0016 which results in a flux correction of <4 per cent at 3729 Å, insignificant compared to the line-measurement errors.

Unlike the Mg II absorbers, the Ca II absorbers do contain significant quantities of dust. However, as argued in WHP06, the quantity of dust, associated errors and resulting obscuration bias are well determined. The $E(B-V)$ values obtained are not dissimilar to those expected from sightlines passing through the discs of spiral galaxies.

However, it is possible, and perhaps likely, that nebular emission-line regions suffer significantly greater dust extinction than that experienced by the majority of the ISM. Bell & Kennicutt (2001) found a median $E(B-V)$ of $\sim$0.4 for nebular emission regions of nearby star forming galaxies, although the mean SFR of their sample is considerably larger than for the systems studied in this paper.

With the currently available data it is only possible to obtain a rough estimate of the true attenuation in the nebular emission regions we observe. By combining all 1559 Mg II absorbers with $z_{\rm abs} < 0.85$, in which Hβ is potentially visible, we find an [O II] to Hβ ratio of 1.9. Given the theoretical balmer decrement (Osterbrock 1989), relation between Hα line strength and SFR (Kennicutt 1998a), and between [O II] line strength and SFR (Kewley et al. 2004), we predict a ratio of 3.44. This suggests dust attenuation may cause us to be underestimating the SFRs by up to a factor of 2, however, we emphasize that an accurate analysis must await further observations.

4.4.3 *Mg II-selected DLAs*

First, we look at the result with perhaps the farthest reaching implications, that the SFR per unit area in DLA gas is observed to be a magnitude lower than that expected from the Schmidt law. We consider in turn the effects of the adopted mean N(H I), DLA fraction, absorber size, contamination by non-DLA absorbers to the measured SFR and dust.

As stated in Section 3.4 it would be very surprising were the mean N(H I) and contamination fraction of our Mg II-selected DLA sample to turn out to be very different from those found by Rao et al. (2006) given the essentially identical criteria used to define both absorber samples. Were we to overestimate the size of the absorbers we would underestimate the SFR per unit area. The scenario in which the absorber size is reduced to bring our result into line with the Schmidt law is discussed in Section 5 and found to be highly implausible.

Turning to the contamination of the sample by non-DLA absorbers, we concluded in Section 3.2 that non-DLAs could have SFRs of $\sim$31–57 per cent that of the DLAs. If, however, the non-DLAs contributed zero SFR to the measured lines our SFR per absorber would increase by only a further 20 and 40 per cent for the low- and high-redshift samples, respectively. Combining the final SFR per unit area of Section 4.2 with the possibility that the non-DLAs in our sample contribute zero flux to the observed lines allows a SFR per unit area of at most $16.6 \pm 0.6(15 \pm 2) \times 10^{-4}\, h^2\, {\rm M}_\odot\, {\rm yr}^{-1}\, {\rm kpc}^{-2}$, i.e. still a factor of 8 (7) below the Schmidt law for the low- (high-) z samples, respectively.

Finally, as discussed in the previous subsection, attenuation of the [O II] line by dust may be our biggest cause of uncertainty, due to the unknown distribution of dust around star-forming regions compared to in the ISM. Allowing for an underestimate of the SFR by a factor of 2, and that the non-DLAs contribute zero flux, would reduce the discrepancy between our results and the Schmidt law to a factor of 4 (3).

Turning now to the SFR density measurements, assuming the Schmidt law holds and allowing for the non-DLA contaminants to contribute zero flux to the measured lines, we find maximum possible contributions of DLA host galaxies to the overall SFR density of the Universe of 10 ± 3 per cent (4 ± 1 per cent). Within the adopted model, an underestimate of the absorber size does not change our results, due to the compensation by the aperture correction (equation 6). Allowing for the possibility that we have underestimated dust attenuation by at most a factor of 2 brings this result to 20 per cent (8 per cent).

4.4.4 *Ca II absorbers*

As with the Mg II-absorbers, an underestimate of the absorber size cannot change our results, provided the Schmidt law applies. Even given the uncertainty in dust extinction, it is difficult to see how the inferred contribution of Ca II absorber host galaxy light, that falls within the $\sim 15\, h^{-1}$ kpc diameter covered by the SDSS-fibres, can contribute more than a few per cent to the global SFR density.

5 DISCUSSION

Given our lack of knowledge concerning the size distribution and geometry of Ca II and DLA absorbers we have, in the previous section, deliberately confined ourselves to providing illustrative calculations of the SFR per unit area and the volume averaged SFR density based on conventional assumptions concerning the size of the absorbers and the relationship between N(H I) and SFR. In particular, no account has been taken of more realistic geometries that may be involved in the relation between the measured N(H I)-column along a single line of sight through an absorber and the spatial distribution of star formation within the system giving rise to the absorber. Further quantitative progress must await the results of imaging

investigations capable of constraining the extent of the star forming regions in Ca II and DLA absorbers at $z \lesssim 1$. However, the detection of weak [O II] $\lambda\lambda$3727,3730 nebular emission associated with the Ca II and Mg II-selected DLA candidate absorbers places strong constraints on the combination of absorber size, space density and star formation properties of absorption-selected systems.

The lower value of dP/dz and the significantly higher SFR seen in the high-redshift Ca II absorbers compared to the Mg II-selected DLA candidate absorbers fits in well with the view advanced in WHP06 that the Ca II absorbers represent chemically evolved systems with detectable quantities of dust that may be spatially closely related to intermediate brightness late-type galaxies. Since the combination of absorber size and SFR produces a SFR per unit area closer to that expected from the Schmidt law, assuming Ca II absorbers have mean N(H I) similar to that found in DLAs, adds further weight to such an interpretation. However, the consequence of this picture is that Ca II absorbers then account for only a small fraction, just $\sim$3 per cent, of the total SFR density in the universe at $z \simeq 0.5$–1. Appealing to a missing fraction of absorbers with associated extinction exceeding our sensitivity limit of $E(B-V) \simeq 0.25$ mag can increase the fractional contribution to the $\dot{\rho}^*$ but not to the extent of explaining the factor of $\sim$30 discrepancy. Indeed, the fraction of 'missing' absorbers required would be inconsistent with established limits on the number of obscured DLA systems at high redshift (Ellison et al. 2001, 2004).

Although the contribution of the low- and high-redshift Ca II samples to the global SFR density is constant, the significant difference between the observed SFR per unit area for the two samples is something of a puzzle. A resolution to the difference awaits the results of imaging studies of the Ca II absorbers and we will report on such observations in the near future.

The low measured SFR associated with the Mg II-selected DLA absorbers results in new constraints on the SFR per unit area and, assuming the absorbers are large ($\gtrsim 9\,h^{-1}$ kpc), on the contribution to the volume averaged SFR density, $\dot{\rho}^*$, of the host galaxy light falling within a $\simeq 7.5\,h^{-1}$ kpc radius of the DLA absorbers. If the absorbers are indeed large, and assuming the Rao et al. (2006) mean value for N(H I), then the SFR per unit area may be as much as an order of magnitude, and certainly a factor of several, below that predicted by the Schmidt law. Correspondingly, the contribution of DLAs to $\dot{\rho}^*$ (at $z \sim 1$) of the universe is dramatically smaller than that deduced by Hopkins et al. (2005), who assumed that the Schmidt law does apply.

It is possible to make our constraints on the SFR per Mg II-selected DLA candidate consistent with the predictions of the Schmidt law, and hence produce a contribution to $\dot{\rho}^*$ as derived by Hopkins et al. (2005), but only by making the individual DLA absorbers very small. Specifically, to bring the SFR per unit area for the Mg II-selected DLA candidate absorbers into agreement with the Schmidt prediction and $\langle N(\mathrm{H\,I})\rangle$ of Rao et al. (2006), the physical size of the absorbers must be $\simeq 3(4)\,h^{-1}$ kpc in radius, where the absorber size comes about by requiring that the surface area of an absorber times the SFR per unit area predicted by the Schmidt law, equals the integrated SFR per absorber we observe (Table 1). The size of the actual regions associated with star formation (i.e. with N(H I) $>5 \times 10^{20}$ cm^{-2}), is then only $\simeq 2(2.5)\,h^{-1}$ kpc in radius. The small physical size of the absorbers then requires that the space density of DLA absorbers at $z \sim 1$ is very large indeed, $\sim 0.13\,h^3$ Mpc^{-3}. A scenario in which such small absorbers are hosted by galaxies of similar space density is inconsistent with the established observation that the bulk of star formation at $z \sim 1$ occurs in luminous galaxies (Hippelein et al. 2003; Bell et al. 2005; Wolf et al. 2005). Alternatively, gaseous galaxy haloes may contain many small DLA absorbers (i.e. have 'filling factors' considerably less than unity), extending far beyond the extent of the SDSS fibre. Such a scenario is, however, inconsistent with observed DLA and associated metal line profiles as many independent components would be visible within the profiles (Wolfe, Gawiser & Prochaska 2005). In summary, reducing the size of the absorbers such that the Schmidt law holds, produces a size/space-density constraint inconsistent with any current favoured model for DLA absorbers and galaxies in general.

Alternatively, the low-redshift Schmidt law may not hold for gas contained in intermediate- to high-redshift quasar absorption-line systems. Recently, Wolfe & Chen (2006) have deduced an upper limit to the SFR per unit area associated with DLA absorbers at redshifts $z = 2.5$–3.5 of less than 10 per cent of that predicted from the Schmidt law. The Wolfe and Chen limit is based on the non-detection of the absorbers in the Hubble ultra-deep field and is therefore a strict *upper* limit. The interpretation of Wolfe and Chen is that in galaxies with low dust and molecular content, as in the DLAs, the threshold H I column density required to trigger star formation is significantly higher than in the nearby galaxies where the empirical Schmidt law was calibrated. Both these results, and the results presented in this paper, are inconsistent with the SFR per unit area derived from C II* by Wolfe et al. (2003a,b), for a full discussion of possible reasons we refer the reader to Wolfe & Chen (2006).

Whatever the physical explanation, it is now difficult to escape the conclusion that only a small fraction of the star formation rate seen directly in galaxy surveys at redshifts from $z = 0.5$ to 3.5 is apparently associated with the relatively large 6–9 h^{-1} kpc region surrounding DLA absorbers. Evidently, the largest contribution to the DLA cross-section is from gas which is too diffuse to support high rates of star formation and metal production, thus explaining the generally low metallicities of most DLAs (e.g. Akerman et al. 2005). However, there are two plausible models consistent with our results. Recent theoretical work by Johansson & Efstathiou (2006) favours extended distributions of DLA gas, with the cross-section dominated by small galaxies, and their predicted mean SFR per DLA host is in very good agreement with the values measured here. Recent observational work at both low and high redshift supports such a scenario: Chun et al. (2006) measure luminosities of low-redshift DLA hosts of $\leqslant 0.1L*$; and Kulkarni et al. (2006) place limits on the SFR of high-redshift DLA hosts of 0.9–2.7 $\mathrm{M}_\odot\ \mathrm{yr}^{-1}$. Alternatively, Wolfe & Chen (2006) associate low surface density H I regions, in which a reduced star formation rate efficiency exists, with the periphery of luminous, star-forming galaxies at $z \simeq 3$. The low-redshift Schmidt law may indeed still apply in the inner regions of these galaxies but the typical host to DLA absorber separation must then exceed the $\simeq 7.5\,h^{-1}$ kpc radius corresponding to the SDSS fibres. It should be relatively straightforward to assess the validity of these models at $z < 1$, where the putative star-forming galaxies associated, but not coincident, with the DLAs should be relatively easy to identify from ground-based images. We have begun such a study and will report on the results in the near future.

ACKNOWLEDGMENTS

We are grateful to Bob Carswell, Hsiao-Wen Chen, Emma Ryan-Weber and Art Wolfe for helpful discussions and to the anonymous referee for suggestions which improved this paper. VW is supported by the MAGPOP Marie Curie EU Research and Training Network.

Funding for the SDSS has been provided by the Alfred P. Sloan Foundation, the Participating Institutions, the National Science

Foundation, the US Department of Energy, the National Aeronautics and Space Administration, the Japanese Monbukagakusho, the Max Planck Society and the Higher Education Funding Council for England. The SDSS Web Site is http://www.sdss.org/.

The SDSS is managed by the Astrophysical Research Consortium for the Participating Institutions. The Participating Institutions are the American Museum of Natural History, Astrophysical Institute Potsdam, University of Basel, Cambridge University, Case Western Reserve University, University of Chicago, Drexel University, Fermilab, the Institute for Advanced Study, the Japan Participation Group, Johns Hopkins University, the Joint Institute for Nuclear Astrophysics, the Kavli Institute for Particle Astrophysics and Cosmology, the Korean Scientist Group, the Chinese Academy of Sciences (LAMOST), Los Alamos National Laboratory, the Max-Planck-Institute for Astronomy (MPIA), the Max-Planck-Institute for Astrophysics (MPA), New Mexico State University, Ohio State University, University of Pittsburgh, University of Portsmouth, Princeton University, the United States Naval Observatory and the University of Washington.

REFERENCES

Adelman-McCarthy J. K., Agüeros M. A., Allam S. S., et al. (The SDSS Collaboration), 2006, ApJS, 162, 38
Akerman C. J., Ellison S. L., Pettini M., Steidel C. C., 2005, A&A, 440, 499
Bell E. F., Kennicutt R. C., 2001, ApJ, 548, 681
Bell E. F., Papovich C., Wolf C. et al., 2005, ApJ, 625, 23
Bergeron J., Boisse P., 1991, A&A, 243, 344
Bolton A. S., Burles S., Schlegel D. J., Eisenstein D. J., Brinkmann J., 2004, AJ, 127, 1860
Bouwens R., Illingworth G., 2006, New Astron. Rev., 50, 152
Chen H.-W., Lanzetta K. M., 2003, ApJ, 597, 706
Chen H.-W., Kennicutt R. C., Rauch M., 2005, ApJ, 620, 703
Chun M. R., Gharanfoli S., Kulkarni V. P., Takamiya M., 2006, AJ, 131, 686
Churchill C., Steidel C., Kacprzak G., 2005, in Braun R., ed., ASP Conf. Ser. Vol. 331, Extra-Planar Gas Mg II Absorbing Galaxies: Morphologies and Kinematics. Astron. Soc. Pac., San Francisco, p. 387
Edgar R. J., Savage B. D., 1989, ApJ, 340, 762
Ellison S. L., Yan L., Hook I. M., Pettini M., Wall J. V., Shaver P., 2001, A&A, 379, 393
Ellison S. L., Churchill C. W., Rix S. A., Pettini M., 2004, ApJ, 615, 118
Ferguson H. C., Dickinson M., Giavalisco M. et al., 2004, ApJ, 600, L107
Hewett P. C., Irwin M. J., Bunclark P., Bridgeland M. T., Kibblewhite E. J., He X. T., Smith M. G., 1985, MNRAS, 213, 971
Hippelein H., Maier C., Meisenheimer K. et al., 2003, A&A, 402, 65
Hogg D., 1999, Distance Measures in Cosmology. Online only reference: astro-ph/9905116
Hopkins A. M., 2004, ApJ, 615, 209
Hopkins A. M., Rao S. M., Turnshek D. A., 2005, ApJ, 630, 108
Hunter I., Smoker J. V., Keenan F., Ledoux C., Jehin E., Cabanac R., Melo C., Bagnulo S., 2006, MNRAS, 367, 1478
Johansson P., Efstathiou G., 2006, MNRAS, 371, 1519
Kennicutt R. C., 1998a, ARA&A, 36, 189
Kennicutt R. C., 1998b, ApJ, 498, 541
Kewley L. J., Geller M. J., Jansen R. A., 2004, AJ, 127, 2002
Lanzetta K. M., Wolfe A. M., Turnshek D. A., 1995, ApJ, 440, 435
Kulkarni V. P., Woodgate B. E., York D. G., Thatte D. G., Meiring J., Palunas P., Wassell E., 2006, ApJ, 636, 30
Le Brun V., Bergeron J., Boisse P., Christian C., 1993, A&A, 279, 33
Le Brun V., Bergeron J., Boisse P., Deharveng J. M., 1997, A&A, 321, 733
Madgwick D. S., Lahav O., Baldry I. K. et al. (The 2dFGRS Team), 2002, MNRAS, 333, 133
Murphy M. T., Liske J., 2004, MNRAS, 354, L31
Osterbrock D. E., 1989, Astrophysics of Gaseous Nebulae and Active Galactic Nuclei. University Science Books, Mill Valey, CA
Peebles P. J. E., 1993, Principles of physical cosmology. Princeton Series in Physics. Princeton University Press, Princeton, NJ
Pei Y. C., 1992, ApJ, 395, 130
Pettini M., King D. L., Smith L. J., Hunstead R. W., 1997, ApJ, 478, 536
Prochaska J. X., Herbert-Fort S., Wolfe A. M., 2005, ApJ, 635, 123
Rao S. M., Nestor D. B., Turnshek D. A., Lane W. M., Monier E. M., Bergeron J., 2003, ApJ, 595, 94
Rao S. M., Turnshek D. A., Nestor D. B., 2006, ApJ, 636, 610
Savage B. D., Sembach K. R., 1996, ARA&A, 34, 279
Schmidt M., 1959, ApJ, 129, 243
Schneider D. P., Hall P. B., Richards G. T., et al. (The SDSS Collaboration), 2005, AJ, 130, 367
Shapley A. E., Steidel C. C., Erb D. K., Reddy N. A., Adelberger K. L., Pettini M., Barmby P., Huang J., 2005, ApJ, 626, 698
Steidel C. C., Dickinson M., Meyer D. M., Adelberger K. L., Sembach K. R., 1997, ApJ, 480, 568
Steidel C. C., Dickinson M., Persson S. E., 1994, ApJ, 437, L75
Trump J. R., Hall P. B., Reichard T. A., 2006, preprint (astro-ph/0603070)
Vladilo G., 2004, A&A, 421, 479
Weatherley S. J., Warren S. J., Møller P., Fall S. M., Fynbo J. U., Croom S. M., 2005, MNRAS, 358, 985
Welsh B. Y., Sasseen T., Craig N., Jelinsky S., Albert C. E., 1997, ApJS, 112, 507
Welty D. E., Morton D. C., Hobbs L. M., 1996, ApJS, 106, 533
Wild V., Hewett P. C., 2005a, MNRAS, 361, L30
Wild V., Hewett P. C., 2005b, MNRAS, 358, 1083
Wild V., Hewett P. C., Pettini M., 2006, MNRAS, 367, 211 (WHP06)
Wolfe A. M., Chen H. W. 2006, ApJ, submitted
Wolfe A. M., Gawiser E., Prochaska J. X., 2003a, ApJ, 593, 235
Wolfe A. M., Prochaska J. X., Gawiser E., 2003b, ApJ, 593, 215
Wolfe A. M., Gawiser E., Prochaska J. X., 2005, ARA&A, 43, 861
Wolf C., Bell E. F., McIntosh D. H. et al., 2005, ApJ, 630, 771
York D. G., Khare P., Vanden Berk D. et al., 2006, MNRAS, 274
Zwaan M. A., van der Hulst J. M., Briggs F. H., Verheijen M. A. W., Ryan-Weber E. V., 2005, MNRAS, 364, 1467

APPENDIX A: CORRECTING THE REDSHIFT PATH FOR THE EFFECT OF DUST ASSOCIATED WITH THE ABSORBERS

The probability of finding an absorption line system intervening in a quasar spectrum depends on the total redshift path between the quasar and us, the S/N of the quasar spectrum and the equivalent width of absorber that we are searching for. The effect of dust in an intervening absorption system is to reduce the S/N of the quasar spectrum, thus reducing the effective redshift path-length that each spectrum provides for finding an absorber of a given EW. The quasar may also be entirely removed from the sample as its magnitude falls below the survey flux limit.

To estimate the total effect of a population of absorbers with known distributions of line equivalent width, dust content and redshift, on the background quasar population of our survey, we simply imagine placing each absorber in front of every one of the input quasars in our survey. We calculate the redshift path available to find a dust-free absorber:

$$(\Delta z)_{j,\text{no-dust}} = \sum_{k,m_k<19.1} \Delta X_k \times P(z_{\text{abs},j}, W_j, m_k) \qquad \text{(A1)}$$

and that available to find a dusty absorber causing A magnitudes of extinction in the observed frame i band:

$$(\Delta z)_{j,\text{dust}} = \sum_{k,m_k+A_j<19.1} \Delta X_k \times P(z_{\text{abs},j}, W_j, m_k + A_j), \qquad \text{(A2)}$$

where the sum is over all quasars brighter than our survey magnitude limit, k denotes a quantity associated with the background quasar

and j a quantity associated with the absorber to be found. ΔX is the redshift path defined by the limits of the survey given in Section 2.1:

$$\Delta X = \min[1.3, z_{\rm qso} - 0.1] - \max\left[0.4, \frac{1250(1+z_{\rm qso})}{2796} - 1\right]. \quad \text{(A3)}$$

The probability, P, of detection of a line of given equivalent width and redshift, in a spectrum of a quasar of given magnitude, is calculated from Monte Carlo simulations: Gaussian line features are placed in the quasar spectra, our initial detection algorithm is run and the rate of recovery of the lines is measured. Including the probability of detection of the Mg II $\lambda\lambda$2796, 2803 doublets has a negligible effect on the final results, due to their being considerably stronger than the Ca II lines (mean equivalent width of $W_{\lambda 2796} = 2.16$ Å).

The extinction in individual absorbers is estimated in the same way as for the subsamples, except that the absorber spectra are not combined into composites before the extinction curve is fitted. While the error on each individual reddening measure is large due to the unknown colour of the background quasar, the observed trends with equivalent width of Ca II give us confidence that on average the correct value is measured.

A correction factor, $\Delta z_{\rm no-dust}/\Delta z_{\rm dust}$, is calculated for each observed absorption-line system, which tells us the number of absorbers missed for each one seen. An estimate is thus obtained of the total number of absorbers missing from our sample. Of course, this method only allows us to estimate correction factors for regions of absorber parameter space which are well sampled by our observations. At high reddening values the number of absorbers drops dramatically and we are unable to correct reliably for absorbers with an $E(B-V) > 0.2$ and > 0.25 for the low- and high-redshift samples, respectively. Our results are therefore only applicable to absorbers with reddening values below these limits. To place these $E(B-V)$ limits into context, the reddening present in galaxies at $z \sim 2$, selected via ultraviolet continuum flux, has a median of 0.15 mag and ranges between 0.0 and 0.4 mag (Shapley et al. 2005).

This paper has been typeset from a TEX/LATEX file prepared by the author.